Analytical and Bioanalytical Chemistry (2023) 415:3503–3513
https://doi.org/10.1007/s00216-023-04740-5

RESEARCH PAPER

Performance evaluation of E-nose and E-tongue combined with machine learning for qualitative and quantitative assessment of bear bile powder

Kelu Lei[1] · Minghao Yuan[1] · Sihui Li[1] · Qiang Zhou[1] · Meifeng Li[1,2] · Dafu Zeng[3] · Yiping Guo[1] · Li Guo[1]

Received: 5 March 2023 / Revised: 6 May 2023 / Accepted: 9 May 2023 / Published online: 18 May 2023

Abstract

Bear bile powder (BBP) is a valuable animal-derived product with a huge adulteration problem on market. It is a crucially important task to identify BBP and its counterfeit. Electronic sensory technologies are the inheritance and development of traditional empirical identification. Considering that each drug has its own specific odor and taste characteristics, electronic tongue (E-tongue), electronic nose (E-nose) and GC-MS were used to evaluate the aroma and taste of BBP and its common counterfeit. Two active components of BBP, namely tauroursodeoxycholic acid (TUDCA) and taurochenodeoxycholic acid (TCDCA) were measured and linked with the electronic sensory data. The results showed that bitterness was the main flavor of TUDCA in BBP, saltiness and umami were the main flavor of TCDCA. The volatiles detected by E-nose and GC-MS were mainly aldehydes, ketones, alcohols, hydrocarbons, carboxylic acids, heterocyclic, lipids, and amines, mainly earthy, musty, coffee, bitter almond, burnt, pungent odor descriptions. Four different machine learning algorithms (backpropagation neural network, support vector machine, K-nearest neighbor, and random forest) were used to identify BBP and its counterfeit, and the regression performance of these four algorithms was also evaluated. For qualitative identification, the algorithm of random forest has shown the best performance, with 100% accuracy, precision, recall and F1-score. Also, the random forest algorithm has the best R^2 and the lowest RMSE in terms of quantitative prediction.

Keywords Bear bile powder · Identification · E-tongue · uf-GC E-nose · GC-MS · Machine learning

Introduction

Bear bile powder (BBP) is an animal-derived product that has been used for thousands of years for the treatment of liver and gallbladder diseases and human health care [1], with the efficacy of protecting liver and bile, dissolving gallstones, anti-cancer, protecting kidney, protecting heart and brain tissue, protecting nerves, suppressing cough and expectorant, treating eye diseases, antibacterial and anti-inflammatory, treating hemorrhoids, regulating intestinal function, regulating immunity, and regulating blood sugar, etc. [2–5]. Bile acids are the main active component of BBP, accounting for more than 70%, of which ursodeoxycholic acid (UDCA) is approved by the US Food and Drug Administration (FDA) as the only drug for the treatment of primary biliary cirrhosis [6, 7]. A recent groundbreaking study has shown that UDCA can prevent SARS-CoV-2 infection [8]. The reason for this is that UDCA blocks the farnesoid X receptor (FXR), which directly reduces the amount of ACE2 on the cell surface, thereby directly blocking the entry of this virus into the cells [8]. Taurolite® has been marketed in Italy for more than 20 years as a first-line cholagogic agent with the chemical composition tauroursodeoxycholic acid (TUDCA), which has demonstrated potent clinical efficacy of choleretic and lithotripsy [9]. In addition, BBP's purgative and hepatoprotective effects are unique to its macromolecular protein components, which have highly effective

✉ Yiping Guo
yguo8@ucmerced.edu

✉ Li Guo
guoli@cdutcm.edu.cn

[1] State Key Laboratory of Southwestern Chinese Medicine Resources, School of Pharmacy, Chengdu University of Traditional Chinese Medicine, No. 1166, Liutai Avenue, Chengdu 611137, China

[2] School of Public Health, Chengdu University of Traditional Chinese Medicine, Chengdu 611137, China

[3] Chengdu Jingbo Biotechnology Co., Ltd, No.39 Renhe Street, Chengdu 611731, China

anti-hepatitis C virus effects that cannot be replaced by other Chinese medicines or synthetic products such as other animal bile and tauroursodeoxycholic acid, for which no effective vaccine or excellent drug has been developed to treat hepatitis C [10, 11].

The extensive clinical demand and irreplaceable unique medicinal value of BBP have built up the huge economic and social benefits of BBP industrialization. However, it is particularly common to find cheap or non-medicinal bile powder adulterated with the expensive BBP due to the great difference in the price [12]. Currently, thin layer chromatography (TLC) and high-performance liquid chromatography (HPLC) methods are the most commonly used methods for BBP identification [6, 13, 14]. However, the preparation procedures of chemical composition analysis are more complex and time-consuming, requiring the purchase of standards and the use of large amounts of organic solvents. Biological methods such as DNA barcoding are accurate and reliable, but complex and time-consuming to operate [15]. Mass spectrometry-based analytical methods, such as liquid chromatography-mass spectrometry coupling [16], and the emerging chip-based nano-electrospray ionization tandem mass spectrometry (nano-ESI-MS/MS) [17]. These techniques can bring a wider range of chemical composition information to BBP, but they are not universally applicable due to high operator requirements, complex sample pretreatment, and difficulties in setting up the chip platform. Our team is dedicated to the research of BBP identification, and has successfully applied Fourier infrared spectroscopy (FT-IR) [18], elemental analysis isotope ratio mass spectrometry (EA-IRMS) and inductively coupled plasma mass spectrometry (ICP-MS) techniques to establish a reliable method for BBP authenticity and origin tracing [11]. Since FTIR, LC-MS, DNA barcoding, ICP-MS and other detection methods have their own advantages and limitations, it is important to find an accurate and effective method for the identification of BBP as a complement, which can reflect the intrinsic quality of BBP as a whole.

Due to their ability to simulate biological senses, electronic nose (E-nose) and electronic tongues (E-tongue) have been widely accepted and adopted in many fields[19–21]. E-nose is a new analytical device that mimics the human olfactory system and is often combined with gas chromatography (GC) or gas chromatography coupled with mass spectrometry (GC-MS) to identify and evaluate the volatile characteristics of a sample [22–24]. E-tongue is an artificial intelligence instrument developed to imitate the human taste system, and has achieved satisfactory results in the application of quality evaluation, geographical origin detection, and adulteration identification of food and Chinese medicine [25–27]. Electronic sensors combined with data fusion to predict the ingredient content have been successfully applied to assess the quality of food and Chinese medicines [28–30]. Additionally, the E-nose and E-tongue technologies are highly automated and easy to operate, making them particularly suitable for market supervision and daily applications. Moreover, the complex and diverse information provided by odor and taste allows for a more comprehensive control of the overall quality of BBP. Compared to chemical-specific analysis, it can prevent misclassification due to artificially added chemical components. However, no relevant studies on BBP have been reported.

Therefore, in this study, objective and accurate electronic sensory techniques and GC-MS analysis were employed based on machine learning to characterize the differences in aroma and taste of BBP and its common counterfeit to help solve the problem of identifying the authenticity of BBP. Further, a reliable pattern recognition method is needed to correlate the tested e-nose and e-tongues signals with identification and content prediction. Commonly used machine learning methods such as random forest (RF), backpropagation neural network (BPNN), K-nearest neighbour (KNN) analysis and support vector machines (SVM) have been combined with sensor technology for food and drug identification and content prediction [31–36]. This study will establish a new method for the overall evaluation of BBP based on its aroma and flavor, as a complementary to other analysis, in the expectation that it will contribute to the market regulation and rapid identification of BBP.

Materials and methods

Sample collection and chemicals

A total of 30 batches of BBP samples and 12 batches of common counterfeit were collected, as detailed in Table S1(see Electronic Supplementary Material Table S1). 21 batches of BBP were from Sichuan Province and were provided by Chengdu Jingbo Biotechnology Co., Ltd. (former Dujiangyan Deer Farm of Sichuan traditional Chinese Medicine Company). The remaining 9 batches of BBP were purchased from common origins (three batches each from Yunnan, Jilin and Fujian origins). 12 batches of common counterfeit were collected from slaughterhouses, including pig bile powder (PBP), cattle bile powder (CBP), sheep bile powder (SBP) and goose bile powder (GBP), and these samples were filtered, dried at 50°C and crushed into powder in the laboratory [11]. All 42 batches of samples were stored in desiccators. The detailed sources of the samples are shown in Table S1 (see Electronic Supplementary Material Table S1). Standards of tauroursodeoxycholic acid sodium salt (batch number PS210615-82, purity≥98%), and taurochenodeoxycholic acid sodium salt (batch number PS210708-16, purity≥98%) were purchased from Chengdu Pusi Biotechnology Co., Ltd.; methanol (HPLC grade) was purchased

from Fisher Scientific Corporation (Loughborough, UK); n-alkane nC6~nC16 mixed reference substance was purchased from RESTEK Company.

Determination of active chemical components in bear bile powder

Since the main bile acids of bear bile were tauroursodeoxycholic acid (TUDCA) and taurochenodeoxycholic acid (TCDCA), we chose these two components as one of the evaluation indexes. The contents of TUDCA and TCDCA in BBP and its common counterfeit were determined according to the standard of BBP issued by Foods and Drugs Administration of Yunnan Province of China (Yun YPBZ-0205-2014). 50mg of samples was extracted with 10 mL of methanol by sonication (240 W, 40 kHz) for dissolution. The sample solutions were filtered with an 0.22 μm syringe filter. The mixed reference solution of TCDCA and TUDCA reference solution of about 1 mg/mL were prepared in methanol and stored at 4°C for later analysis. The HPLC analyses were performed with a Dionex UltiMate 3000 series equipped with an UltiMate 3000 Quaternary Pump, an UltiMate 3000 Autosampler, an UltiMate 3000 Column compartment, an Ultimate 3000 Diode Array Detector, and a Chromeleon 7 chromatography workstation (Thermo Fisher Scientific, Waltham, MA, USA). An Agilent Eclipse XDB-C18 column (150 mm × 4.6 mm, 5 μm) was used. The solution (sodium dihydrogen phosphate 4.68 g and sodium heptanesulfonate 2.0 g dissolved in 400 mL water, then added 600 mL methanol, shaken well) was used as mobile phase A, methanol was used as mobile phase B, the gradient program as follow: 100% A for 0~8min, and 90%A for 8~23min. The flow rate was maintained at 1.0 mL/min and the detective wavelength was selected at 205 nm. The column temperature was 30 °C and the injection volume was 10 μL.

Electronic tongue analysis

The taste-sensing system SA402B (Intelligent Sensor Technology Co. Ltd, Atsugi, Japan) consisted of sensor array, detection instrument, and the operating computer. The sensor array was equipped with five lipid membrane sensors, enabling the evaluation of four basic tastes (umami, saltiness, sourness, bitterness), and four aftertaste values, namely aftertaste-astringency (aftertaste-A), aftertaste-bitterness (aftertaste-B), stringency, and richness of taste [37]. The artificial lipid membrane sensor probe was consisted of silver wire electrodes coated with Ag/AgCl, the sensor body was made of polypropylene, and the lipid membranes was made by mixing lipids (which play an important role in taste sensing) with a polymer [30]. The reference solution (artificial saliva) was prepared by dissolving 30 mM potassium chloride and 0.3 mM tartaric acid in distilled water for sensor conditioning and cleaning. The washing solutions for positively charged sensors (AE1, C00) were made with 100 mM potassium chloride and 10 mM potassium hydroxide with 30 % ethanol, for the negatively charged sensors (BT0, AN0) were made with 100 mM hydrochloric acid dissolved in 30% ethanol [23]. The taste sensors of the E-tongue have the same thresholds as humans, with quinine hydrochloride, monosodium glutamate and sodium chloride as standard substances representing the four basic tastes of bitterness, sour, umami and saltiness with thresholds of 1E-3 mM, 0.01 mM, 0.05 mM,0.5 mM, respectively [38]. To ensure the reliability and stability of the collected data, the E-tongue should be self-checked, activated, calibrated and diagnosed before measurement. The sensor was placed in the reference solution for 30 seconds, then the measurement began. Each sample was repeated 4 times, and the last 3 times were taken as test results to ensure data stability.

Electronic nose analysis

Ultrafast gas chromatography electronic nose (uf-GC E-nose) (Heracles II, Alpha MOS, Toulouse, France) was used, equipped with a HS100 auto-sampler, a sorption trap, an injector, two FID detectors, and two independent chromatographic columns with a non-polar column was MTX- 5 (10 m × 0.18 mm, 0.4 μm film thickness) and a medium polar column was MXT- 1701 (10 m × 0.18 mm, 0.4 μm film thickness) [39]. Heracles II uf-GC E-nose, a new type of odor analysis instrument, had the advantages of sensitive detection and very short analysis time with a detection limit of nC_{12} < 100 pg [40]. It also had a reliable repeatability with RSD < 0.3% for retention time and RSD < 3% for peak area [40]. It could be used as a sensor of the chromatographic peak obtained from the gas phase, replacing the limited sensory signal of the traditional sensor-based electronic nose for more compound signals. After converting retention time to Kovats retention index and alibration by n-alkanes qualitative analysis through AroChemBase database of AlphaSoft V14.2 software, information on possible compounds and their corresponding sensory descriptions could be obtained, which could facilitate further in-depth study of their properties [41]. The experimental conditions of the electronic nose were as follows: 0.5 g of the sample was weighed into the headspace injection vial, sealed with a cap, and analyzed under the instrument parameter settings in Table S2 (see Electronic Supplementary Material Table S2).

GC-MS analysis

Since GC-MS has higher resolution and accuracy for complete identification and quantification of complex samples, which can further complement the results of uf-GC E-nose. An Agilent 7890A gas chromatograph equipped with a mass

spectrometer (model 5975C, Agilent Technologies, Santa Clara, CA) was used to quantify volatile compounds of BBP and its common counterfeit. The capillary column used was an HP-5MS quartz column (0.25 mm×30 m× 0.25 μm) from Agilent Technologies. The flow rate of the carrier gas (helium, 99.999%) was 1 mL/min, with a shunt ratio of 20:1. The MS conditions were as follows: electron bombardment ion source (EI) with a temperature of 230 °C, fourth-stage rod temperature 150 °C, and electron energy 70 eV. The chromatogram was recorded by monitoring the total ion currents in the m/z range of 50–550. The temperature program was as follows: the initial temperature was set at 60 °C for 2 min, then ramped up to 160 °C at 5 °C/min, and finally to 240 °C at 4 °C/min. The volatile compounds were identified by comparing their MS spectra with those in the NIST14 libraries [24].

Statistical analysis and machine learning models

Random Forest (RF)

Random forest (RF) is a relatively new integrated learning method for machine learning models, which operates by constructing multiple decision trees at different training times, with the output represented as class patterns (classification) or average predictions (regression) of individual trees [34]. For classification, the voting method is usually used, where the most voted category or one of the categories is the final model output; for regression, the simple averaging method is usually used, where the regression results obtained by T weak learners are arithmetically averaged to make the final prediction [35]. RF is to build a forest in a random way, and the forest consists of many unrelated decision trees. In the 1980s, Breiman et al. invented the classification tree algorithm to classify or regress data by repeatedly dichotomizing them, which greatly reduces the computational effort [42]. In 2001, Breiman combined the classification trees into a random forest, i.e., randomized in the use of variables (columns) and data (rows) to generate many classification trees, and then aggregated the classification tree results [43].

Backpropagation neural network (BPNN)

Backpropagation neural network (BPNN), proposed by Rumelhart and McClelland in 1986, is a multilayer forward neural network trained according to an error backward propagation algorithm [44]. BPNN is a very widely used supervised learning network model and belongs to a type of feedforward neural network. Its output results are propagated forward and the errors are propagated backward. The back propagation algorithm continuously adjusts the network weights of the connected neurons by iterative processing, so that the error between the final output and the expected result is minimized [45] .

K-nearest neighbour (KNN)

The k-nearest neighbor (KNN) is a machine learning algorithm for classification and regression with supervised nonparametric methods. Among all machine learning algorithms, KNN is one of the simplest forms and is widely used for classification tasks because of its very adaptive and easy-to-understand design [46]. KNN is able to classify the dataset using a training model similar to the test query by considering the k nearest training data points (neighbors) that are closest to the query it is testing. Finally, the algorithm performs a majority voting rule to check the classification to be finalized. The class with the most occurrences is ruled as the final classification for the query [47].

Support vector machine (SVM)

Support vector machines (SVM) creates a machine learning theory based on Vapnik-Chervonenkis dimensionality theory and structural risk minimization principles [48].SVM is commonly used for sample classification and regression and are a supervised learning model based on the concept of decision planes [49]. Support Vector Regression (SVR) is a model that uses SVM to fit curves and do regression analysis. Classification and regression problems are the two most important types of tasks in supervised machine learning. Unlike classification where the output is a finite number of discrete values, the output of a regression model is continuous over a range of values [50].SVM algorithms have applications in pattern recognition, regression estimation, and probability density function estimation, and the algorithms have surpassed or are comparable to traditional learning algorithms in terms of efficiency and accuracy.

Before building the model, the sample information was preprocessed using the data shuffling method, and the dataset was randomly divided into 70% and 30% for model training and testing, respectively, and then 8 and 6 samples were selected as validation datasets for the classification and regression models, respectively. The parameters of the four machine learning models are shown in Table S3 (see Electronic Supplementary Material Table S3).

The above methods were implemented via PC programming using Python language and SPSSPRO online data analysis platform (https://www.spsspro.com/). SPSS 22.0 (SPSS Inc., Chicago, USA) was used for Pearson correlation analysis and One-way ANOVA. The data obtained in this study were statistically analyzed by Microsoft Excel 2019, and plotted by Origin 2022 (OriginLab, Northampton, MA, USA).

Results and discussion

Composition analysis of bear bile powder

Thirty batches of BBP samples and 12 batches of common counterfeit were tested (see Electronic Supplementary Material Table S4). The HPLC chromatograms for BBP samples and its common counterfeit and pure standards were presented in the Figure S1 (see Electronic Supplementary Material Figure S1). A wide range of BBP was selected for this study, involving samples from four different origins as well as five different years to ensure the accuracy of the experiment. The mean and standard deviation of TUDCA for 30 batches of BBP was 33.085 ± 8.580 % (W/W) and for TCDCA was 30.306 ± 7.605 % (W/W). 12 batches of common counterfeit did not detect the TUDCA component. Among them, the TCDCA content of GBP is the highest, about 1.6 times that of BBP, while the rest of the counterfeit have a very low TCDCA content, about 1/15 to 1/6 of BBP.

Taste profile of bear bile powder

As seen from the radar plot Fig. 1a, with the increase of concentration (0.05~0.8 g/100mL), the response of the sensor and the taste value was moderate at 0.1 g/100mL. Therefore, the experimental conditions for the E-tongue were as follows: 0.1 g of BBP and its common counterfeit were taken, dissolved it in distilled water to 100 mL, removed 30 mL of the test solution and added it into the special sample cup for the E-tongue.

After converting the membrane potential values measured by the E-tongue to taste values according to the Weber-Fechner law (perceived intensity is proportional to the logarithm of the stimulus intensity), the taste values of 30 batches of BBP and 12 batches of common counterfeit were shown in Table S4 (see Electronic Supplementary Material Table S4). Since the data of taste indicators in the samples to be tested were based on the output value of the reference solution as a blank control (i.e., the tasteless point), the tasteless point of sour taste was defined as -13, the tasteless point of salty taste was -6, and the rest of the taste indicators were based on 0 value as the tasteless point. Below the tasteless point was considered to be the absence of the taste. Thus, 30 batches of BBP and 12 batches of common counterfeit had no sour taste, and 12 batches of common counterfeit had no rich taste. As shown in Table S4 and Fig. 2b, 30 batches of BBP and 12 batches of common counterfeit had similar tastes overall, but BBP had lower bitterness, higher umami and saltiness values and a unique richness. The bitter taste may be related to its bile acids, the umami may be related to its amino acids, and the salt taste may be related to the need for bears to lick salt bricks during feeding to maintain electrolyte balance and to replenish minerals needed for their growth and development.

Aromatic features of bear bile powder

Based on the separation of two columns using uf-GC E-nose, the gas chromatograms of BBP and its common counterfeit were shown in Figure S2 (see Electronic Supplementary Material Figure S2). By integrating the uf-GC E-nose chromatography, 35 and 25 peaks were obtained on the MXT-5 and MXT-1701 columns, respectively. According to the AroChemBase database, the possible compounds corresponding to the characteristic peaks of the uf-GC E-nose are shown in Table S5 (see Electronic Supplementary Material Table S5). From the radar plot of odor information Fig. 2b-c, it was clear that the odor information was richer for retention times of 20-30 min

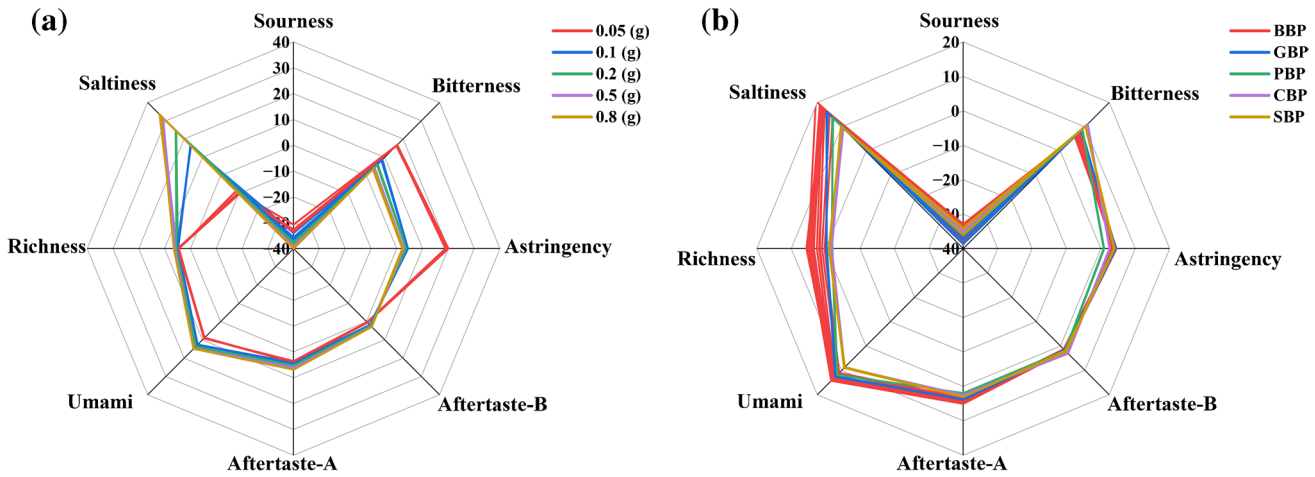

Fig. 1 **a** Radar plot of taste information of BBP with different sampling quantity and **b** Taste radar plot of BBP and its common counterfeit

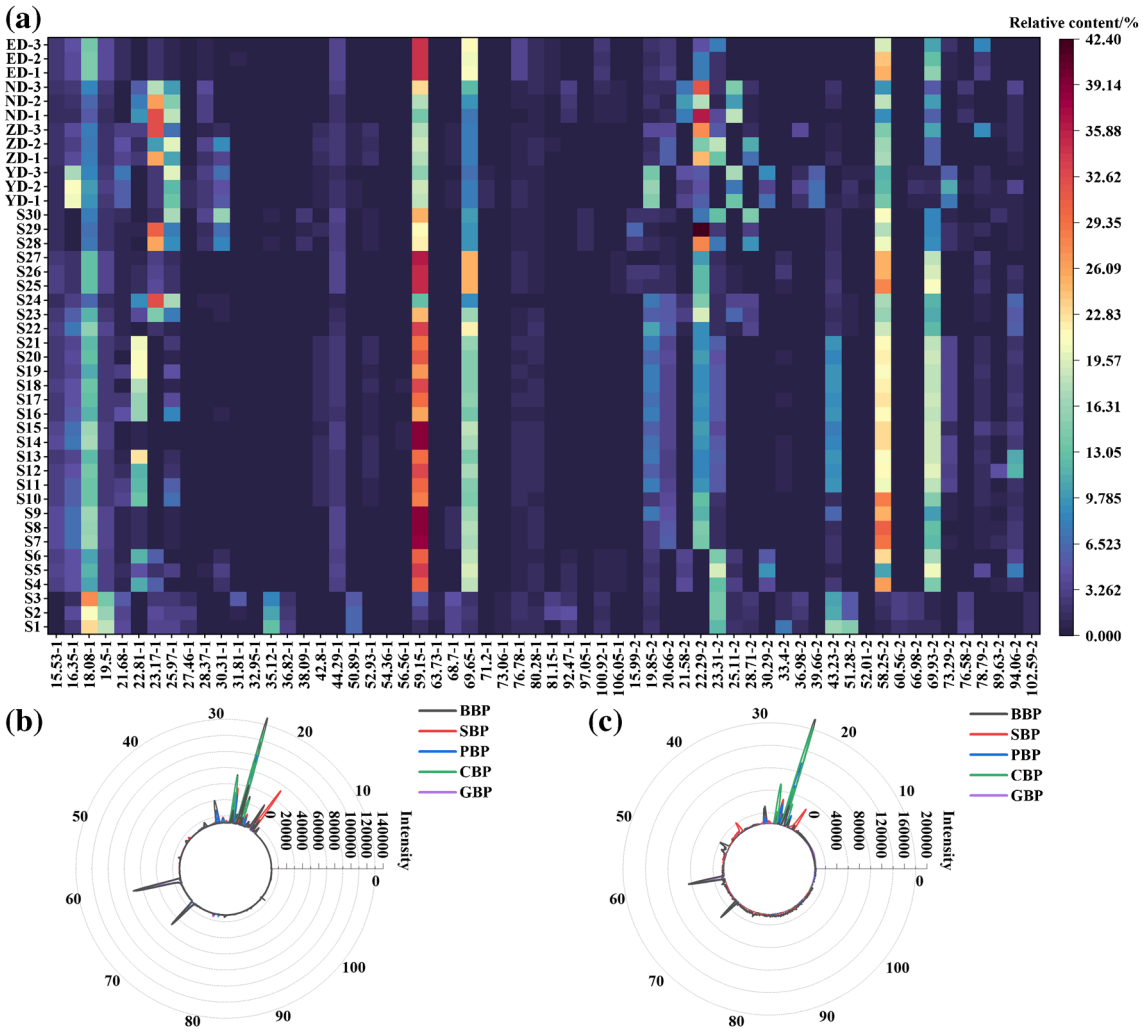

Fig. 2 **a** Odor information based on retention time-relative content (t-ω) data set, the numbers 1 and 2 are added after the retention time to indicate MXT-1701 columns and MXT-5 columns, respectively, BBP had nine significant response points (18.08-1, 22.81-1, 59.15-1, 69.65-1, 19.85-2, 22.29-2, 43.23-2, 58.25-2, 69.93-2), which were significantly different from its common counterfeit in terms of content.; **b** radar plots of BBP and its common counterfeit for column MXT-5 and **c** for column MXT-1701, BBP had richer odor information with retention times of 20-30 min and 60-70 min on both columns

and 60-70 min on both columns. Relative content was obtained by calculating the area ratio for each peak (i.e., the ratio of the area of each compound to the total peak area). The retention time-peak area (t-A) data set was converted to retention time-relative content (t-ω) data set Fig. 2a. Since there were 2 columns, the numbers 1 and 2 were added after the retention time to show the difference, e.g., 15.53-1 and 15.99-2 represent the peak information of retention time 15.53s on column MXT-5 and the peak information of retention time 15.99s on column MXT-1701, respectively. Fig. 2a illustrated the relative contents of BBP and its common counterfeit at the corresponding retention times. As shown in Fig. 2a, BBP had nine significant response points (18.08-1, 22.81-1, 59.15-1, 69.65-1, 19.85-2, 22.29-2, 43.23-2, 58.25-2, 69.93-2), which were significantly different from its common counterfeit in terms of content. After database comparison, the nine characteristic peaks corresponded to the possible compounds of pentane, 3-methylfuran, 2,4,5-trimethylthiazole, valerate, 2-methylpentane, 2-propanol, 2,4-octadiene, octamethylcyclotetrasiloxane and 5-ethyldecane, which provided important information for the identification of bear bile powder from its common counterfeit. After converting the retention times to Kovats retention indices, the qualitative results were obtained from the AroChemBase database and the compounds with correlation indices >80 were shown in Table S6 (see Electronic Supplementary Material Table S6) [41, 51]. BBP, CBP, SBP, GBP and PBP obtained 16,13,24,17 and 12 compounds, respectively. Most of these compounds showed odors such

as earthy, musty, coffee, bitter almond, burnt and pungent, which were consistent with the bitter and pungent odors of animal bile.

The BBP and its common counterfeit were further detected and analyzed by GC-MS technique. Due to the relatively low resolution of uf-GC E-nose, it could only provide odor identification and sensory description of compounds. In contrast, GC-MS has higher sensitivity and accuracy, and could determine the structure and content of compounds. Therefore, GC-MS was used for further detection and analysis of volatile compounds of BBP and its common counterfeit. The total ion chromatogram of GC-MS was shown in Figure S3 (see Electronic Supplementary Material Figure S3). A spectral library of NIST 14 was searched and matched using data obtained from qualitative analysis of the compounds, and substances with a match of more than 80% were selected. The relative content of volatile compounds was expressed using the peak area normalization method. After qualitative and quantitative analysis by GC-MS, 87 components were identified, which were mainly aldehydes, ketones, alcohols, hydrocarbons, carboxylic acids, heterocycles, lipids, amines and a few other compounds (see Electronic Supplementary Material Table S7). 54 components were identified for BBP, 15 components for GBP, 24 components for SBP, 30 components for PBP and 22 components for CBP. BBP and its common counterfeit had 6 common components, 31 components were unique to BBP. Among the common components, 3-(hydroxymethyl)nonan-2-one, decamethylcyclopentasiloxane, octadecamethylcyclononasiloxan and 2,6-dimethylpyrazine of BBP were significantly different from the counterfeit ($P < 0.05$). These components could be used as one of the important indicators to distinguish the BBP from the common counterfeit. Furthermore, compounds such as 3-methylbutyraldehyde, octamethylcyclotetrasiloxane, octane, 2,6-dimethylpyrazine, methylcyclohexane, 1-octene, camphor and hexanoic acid were also detected in the E-nose, indicating that GC-MS could further validate and complement the results of the E-nose.

Correlation analysis based on sensory value and active ingredient content

Pearson correlation analysis was performed between the taste values of BBP and the content of active ingredients, the results were shown in Figure 3. TUDCA was significantly positively correlated with bitterness ($r = 0.75$; $P<0.01$) and negatively correlated with astringency of BBP ($r = -0.47$, $P<0.01$), TCDCA was significantly positively correlated with saltiness and umami ($r = 0.75, 0.71$; $P<0.01$), and negatively correlated with bitterness and aftertaste-B ($r = -0.58$, -0.51; $P<0.01$). From the above results, it can be inferred that the higher the TUDCA content in BPP, the stronger the bitterness, while the higher the TCDCA content, the weaker the bitterness. These results indicated that the bitterness and saltiness taste of BBP mainly originated from bile acids, with TUDCA contributing the most to the bitterness and TCDCA contributing the most to the saltiness. The bitterness of bile acids may be intended to stimulate the intestinal wall to recognize signals for digestion and absorption of fats, while the saltiness may result from the metabolism of bile acids in the body and the combination with other substances to form salts.

Furthermore, the relationship between the odor characteristic peaks of BBP and the two active ingredients was analyzed. The results of the characteristic peaks with the top correlation coefficients were shown in Figure S4 (see

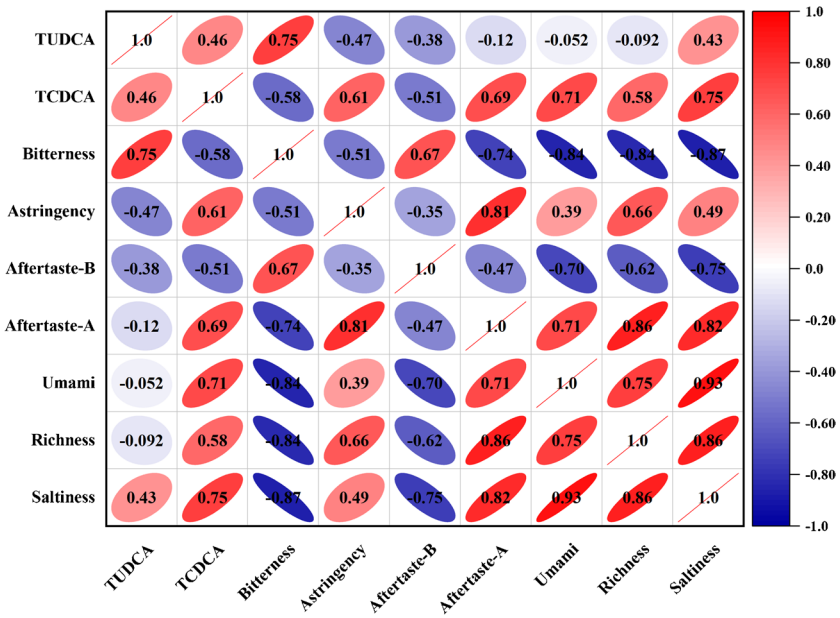

Fig. 3 Pearson correlation analysis based on taste values with two active ingredients of BBP. TUDCA had significant positive correlations with peaks 58.25-2, 56.56-1 and 59.15-1 ($r = 0.75, 0.69, 0.68$; $P<0.01$). TCDCA was significantly positively correlated with saltiness and umami ($r = 0.75, 0.71$; $P<0.01$)

Electronic Supplementary Material Figure S4). TUDCA had significant positive correlations with peaks 58.25-2, 56.56-1 and 59.15-1 with correlation coefficients of 0.75, 0.69 and 0.68, respectively, and were significant at the $P<0.01$ level. In addition, there was a significant positive correlation between TCDCA and peak 27.46-1 ($r = 0.63$, $P<0.01$). It is indicated that the odor of TUDCA may be related to Benzaldehyde, 2,4,5-trimethylthiazole and Octamethylcyclotetrasiloxane, and the odor of TCDCA may be related to 3-methylbutanal.

Comparison of classification and regression properties based on four machine learning models

Four machine learning algorithms based on RF, BPNN, KNN and SVM were used for classifying BBP and common counterfeit. The correct classification for the positive class was True Positive (TP); the incorrect prediction for the negative class was False Negative (FN); the incorrect prediction for the positive class was False Positive (FP); and the correct classification for the negative class was True Negative (TN) [52]. Accuracy was the ratio of the number of samples correctly classified by the classifier to the total number of samples, accuracy = TP/(TP + FP); recall = TP/(TP + FN); F1 score= (2×precision×recall)/(precision+recall) [53]. 70% of the samples were randomly selected as the training subset, 30% as the test subset, and then 6 BBP and 2 counterfeit samples were selected as the validation set. The comparison results of the four machine learning models were shown in Table 1. For classification properties, RF and BPNN showed excellent performance. RF correctly classified BBP with the four counterfeits in the training subset, test subset and validation subset, with a correct rate of 100%. In contrast, KNN and SVM performed relatively poorly in this classification model, with error rates of 25% and 12.5%, respectively. For regression models, R^2 was used to evaluate the goodness of fit, while root mean square error (RMSE) was used to measure the deviation between observed values and true values. They are typically used to assess the predictive performance of machine learning models. RF still showed the best performance in regression model (see Electronic Supplementary Material Table S8 and Figure S6). In the TUDCA quantitative prediction model, the R^2 was 0.95, 0.90, and 0.97 for the training, testing and validation subset, respectively; and the RMSE was 1.82, 1.97, and 2.30, respectively.

The reasons might be as follows. SVM was commonly used for binary classification algorithm, which was not ideal for multi-classification problem solving [54]. SVR had high R^2 and low RMSE only in the training subset, but its testing subset had the worst performance among the four machine learning models. This may be due to the insufficient sample size in this study, while SVR was applicable when the number of samples was smaller than the number of features [55]. Since KNN was a highly distance-dependent algorithm, it was not very good at processing multidimensional data [56]. The data fusion of E-nose and E-tongue in this study had a total of 67 variables, which greatly affected the accuracy of the KNN algorithm. In addition, it is important to choose the appropriate K-value when using the KNN algorithm. If the selected K value is too small, the model is susceptible to overfitting due to noise, while if the selected K value is too large, the model may be underfitted and fail to capture the complexity and variability of the data [57]. Therefore, a genetic algorithm was used to filter the K values from 2 to 20 and to obtain the best value of 5 [58–60]. The R^2 value of KNN was low in all subsets and also had a high RMSE. This may be due to the fact that the prediction results of KNN were susceptible to noise containing data. When the samples contain outliers, the categories of the new samples were biased toward the category with the dominant number in the training sample, which easily lead to prediction errors [61]. The regression fit of BPNN in the test subset was not good enough, which may be due to the insufficient samples, with R^2 of only 0.77 and 0.63 for TUDCA and TCDCA, respectively. The BPNN algorithm was influenced by the complexity of the network structure and the complexity of the samples. As the training ability increased, the prediction ability decreased and the phenomenon of "over-learning" or "under-generalization" occurred [62]. RF had the effect of explaining up to several thousand variables and therefore performed best in this study [63]. RF performed well on the test subset due to the integrated algorithm, which had better accuracy than most individual algorithms. Additionally, the introduction of two randomnesses (sample randomization

Table 1 Summary of the training, testing and validation classification results of the four machine learning models, results are presented in percentages (%)

	Training subset				Testing subset				Validation subset				
	Accuracy	Precision	Recall	F1- score	Accuracy	Precision	Recall	F1- score	Accuracy	Precision	Recall	F1- score	Error rate
RF	100	100	100	100	100	100	100	100	100	100	100	100	0
BPNN	100	100	100	100	92.3	85.3	92.3	88.6	100	100	100	100	0
KNN	79.3	63.4	79.3	70.3	76.9	59.2	76.9	66.9	75	56.25	75	64	25
SVM	100	100	100	100	84.6	94.9	84.6	87.6	87.5	93.75	87.5	89	12.5

and feature randomization) made the random forest less prone to overfitting [64, 65]. A summary of variable importance results based on RF algorithm were displayed in Figure S5 (see Electronic Supplementary Material Figure S5), showing which characteristic variables contribute the most to the model. The results of variable importance for RF showed that bitterness and 56.56-1 are the largest contributing variables for the TCDCA and TUDCA regression models with 9.10% and 12.4%, respectively. Saltiness contributed the most to the classification model of the RF algorithm with 10.8%, which could be used as a discriminatory marker.

Conclusions

In this study, E-tongue, E-nose and GC-MS techniques were used as alternative methods to traditional empirical identification to elaborate the intrinsic components of aroma and taste of BBP. TUDCA and TCDCA were the two main components and active ingredients of BBP. Bitterness was the main taste of TUDCA in BBP, saltiness and umam were the main taste of TCDCA. Moreover, the higher the TUDCA content in BBP, the stronger the bitterness, but the higher the TCDCA content, the weaker the bitterness. BBP had high intensity of odor information on both two columns of uf-GC E-nose with retention times of 20-30 min and 60-70 min. Compared with AroChemBase database, these compounds were related to earthy, musty, coffee, bitter almond, burnt, pungent, etc., consistent with the bitter, pungent, fishy odor of animal bile. GC-MS was performed for the quantitative and qualitative analysis of volatile compounds of BBP and its common counterfeit, mainly ketones, alcohols, carboxylic acids, hydrocarbons, heterocycles compounds, among which the relative content of hydrocarbons was the highest.

Four machine learning algorithms (RF, BPNN, KNN and SVM) are introduced to build classification and regression models and compare their performance according to the statistical parameters of R^2 and RMSE. Data fusion of signals from the E-tongue and E-nose was utilized in the modeling. It was concluded that for qualitative identification, RF achieved perfect classification results with an accuracy of 100%. This was followed by BPNN with 92.3% accuracy in the test subset and 100% in the training and validation subsets. The KNN algorithm performed the worst in the classification results. In terms of quantitative prediction, RF still had the best model prediction ability with R^2 of 0.95, 0.90, and 0.97 for the training set, test set, and validation set, respectively; and RMSE of 1.82, 1.97, and 2.30, respectively. The regression ability of the other three machine learning models in this dataset was not satisfactory. This study showed that E-nose and E-tongue combined with machine learning algorithms could be successfully applied to qualitative and quantitative assessment of BBP, providing new ideas for the identification and analysis of BBP, and new methods for quality control and market supervision of BBP.

Supplementary Information The online version contains supplementary material available at https://doi.org/10.1007/s00216-023-04740-5.

Acknowledgments The authors gratefully acknowledge the E-nose experiment platform supported by Chengdu Institute for Food and Drug Control.

Funding This research was funded by Xinglin Scholars Discipline Talent Research Promotion Plan (Grant No. CXTD2018012) and Xinglin Scholar Research Promotion Project of Chengdu University of TCM (Grant No.030058179), Research and Development of Bear Bile and Plum Deer Series Products (Grant No.301020046).

Declarations

Conflicts of Interest The authors declare no conflict of interest.

References

1. Chen H, Al S, Liu L, Peng J, Chu J. Bear Bile Powder Inhibits Growth of Hepatocellular Carcinoma via Suppressing STAT3 Signaling Pathway in Mice. Chinese J Integ Med. 2020;26(5):370–4. https://doi.org/10.1007/s11655-019-3010-1.
2. Xingling C, Shulan S, Rui L, Dawei Q, Liling C, Liping Q, et al. Chemical constituents and pharmacological action of bile acids from animal: a review. China Journal of Chinese Materia. Medica. 2021;46(19):4898–906. https://doi.org/10.19540/j.cnki.cjcmm.20210630.201.
3. Cai J, Wu J, Fang S, Liu S, Wang T, Li Y, et al. Cultured bear bile powder ameliorates acute liver injury in cholestatic mice via inhibition of hepatic inflammation and apoptosis. J Ethnopharmacol. 2022;284:114829. https://doi.org/10.1016/j.jep.2021.114829.
4. Hofmann AF, Hagey LR. Key discoveries in bile acid chemistry and biology and their clinical applications: history of the last eight decades. J Lipid Res. 2014;55(8):1553–95. https://doi.org/10.1194/jlr.R049437.
5. Lei K, Yuan M, Zhou T, Ye Q, Zeng B, Zhou Q, et al. Research progress in the application of bile acid-drug conjugates: A "trojan horse" strategy. Steroids. 2021;173:108879. https://doi.org/10.1016/j.steroids.2021.108879.
6. Xiong J, Zheng TJ, Shi Y, Wei F, Ma SC, He L, et al. Analysis of the fingerprint profile of bioactive constituents of traditional Chinese medicinal materials derived from animal bile using the HPLC-ELSD and chemometric methods: An application of a reference scaleplate. J Pharm Biomed Anal. 2019;174:50–6. https://doi.org/10.1016/j.jpba.2019.05.035.
7. Huang F, Pariante CM, Borsini A. From dried bear bile to molecular investigation: A systematic review of the effect of bile acids on cell apoptosis, oxidative stress and inflammation in the brain, across pre-clinical models of neurological, neurodegenerative and neuropsychiatric disorders. Brain Behav Immun. 2022;99:132–46. https://doi.org/10.1016/j.bbi.2021.09.021.
8. Brevini T, Maes M, Webb GJ, John BV, Fuchs CD, Buescher G, et al. FXR inhibition may protect from SARS-CoV-2 infection by reducing ACE2. Nature. 2022; https://doi.org/10.1038/s41586-022-05594-0.
9. Feng R, Li J, Chen J, Duan L, Liu X, Di D, et al. Preparation and toxicity evaluation of a novel nattokinase-tauroursodeoxycholate

complex. Asian J Pharm Sci. 2018;13(2):173–82. https://doi.org/10.1016/j.ajps.2017.11.001.
10. Wang XJ, Yan GL, Zhang AH, Sun H, Piao CY, Li WY, et al. Metabolomics and proteomics approaches to characterize and assess proteins of bear bile powder for hepatitis C virus. Chin J Nat Med. 2013;11(6):653–65. https://doi.org/10.1016/s1875-5364(13)60076-x.
11. Yuan M, Gong S, Liu Y, Li X, Li M, Zeng D, et al. Rapid discrimination of the authenticity and geographical origin of bear bile powder using stable isotope ratio and elemental analysis. Anal Bioanal Chem. 2022; https://doi.org/10.1007/s00216-022-04413-9.
12. Jie W, Aizhen X, Rongrong C, Li Y, Zhengtao W, Shaoyong L. Systematical analysis of multiple components in drainage bear bile powder from different sources. China Journal of Chinese Materia. Medica. 2018;43(11):2326–32. https://doi.org/10.19540/j.cnki.cjcmm.20180125.001.
13. Görög S. Identification in drug quality control and drug research. TrAC Trends Analy Chem. 2015;69:114–22. https://doi.org/10.1016/j.trac.2014.11.020.
14. Zhu R, Pu Y. Study on thin-layer chromatographic method for the analysis of bear bile. Gansu Med J. 2015;34(06):459–60. https://doi.org/10.15975/j.cnki.gsyy.2015.06.027.
15. Na T, Yuan Y, Yan J, Quan Y, Tian Z, Jun-de L, et al. DNA fingerprinting identification of bile power(bile) medicines. China Journal of Chinese Materia. Medica. 2020;45(05):1064–9. https://doi.org/10.19540/j.cnki.cjcmm.20200105.106.
16. Qiao X, Ye M, Pan DL, Miao WJ, Xiang C, Han J, et al. Differentiation of various traditional Chinese medicines derived from animal bile and gallstone: simultaneous determination of bile acids by liquid chromatography coupled with triple quadrupole mass spectrometry. J Chromatogr A. 2011;1218(1):107–17. https://doi.org/10.1016/j.chroma.2010.10.116.
17. Zhang Y, Wei J, Li L, Liu Y, Sun S, Xu L, et al. Rapid identification of bear bile powder from other bile sources using chip-based nano-electrospray ionization tandem mass spectrometry. Rapid Commun Mass Spectrom. 2022;36(15):e9326. https://doi.org/10.1002/rcm.9326.
18. Ming-hao Y, Tao Z, Wen-xiao Z, Qiang Z, Ke-lu L, Da-fu Z, et al. Rapid detection of authenticity and adulteration of bear bile powder by FTIR spectroscopy combined with chemometrics. Nat Prod Res Dev. 2022;34(05):856–63. https://doi.org/10.16333/j.1001-6880.2022.5.015.
19. Tan J, Xu J. Applications of electronic nose (e-nose) and electronic tongue (e-tongue) in food quality-related properties determination: A review. Artificial Int Agricul. 2020;4:104–15. https://doi.org/10.1016/j.aiia.2020.06.003.
20. VR N, Mohapatra AK, VK U, Lukose J, Kartha VB, Chidangil S. Post-COVID syndrome screening through breath analysis using electronic nose technology. Analytical and Bioanalytical Chemistry. 2022;414(12):3617–24. https://doi.org/10.1007/s00216-022-03990-z.
21. Jo Y, Chung N, Sw P, Noh BS, Jeong Y-J, Kwon J-H. Application of E-tongue, E-nose, and MS-E-nose for discriminating aged vinegars based on taste and aroma profiles. Food Sci Biotechnol. 2016;25(5):1313–8. https://doi.org/10.1007/s10068-016-0206-4.
22. Long Q, Li Z, Han B, Gholam Hosseini H, Zhou H, Wang S, et al. Discrimination of Two Cultivars of Alpinia Officinarum Hance Using an Electronic Nose and Gas Chromatography-Mass Spectrometry Coupled with Chemometrics. Sensors (Basel). 2019;19(3) https://doi.org/10.3390/s19030572.
23. Zhang X, Wu H, Lin L, Du X, Tang S, Liu H, et al. The qualitative and quantitative assessment of xiaochaihu granules based on e-eye, e-nose, e-tongue and chemometrics. J Pharm Biomed Anal. 2021;205:114298. https://doi.org/10.1016/j.jpba.2021.114298.
24. Yu H, Xie T, Xie J, Ai L, Tian H. Characterization of key aroma compounds in Chinese rice wine using gas chromatography-mass spectrometry and gas chromatography-olfactometry. Food Chem. 2019;293:8–14. https://doi.org/10.1016/j.foodchem.2019.03.071.
25. Ding J, Gu C, Huang L, Tan R. Discrimination and Geographical Origin Prediction of Cynomorium songaricum Rupr. from Different Growing Areas in China by an Electronic Tongue. J Anal Meth Chem. 2018;2018:5894082. https://doi.org/10.1155/2018/5894082.
26. He X, Yangming H, Gorska-Horczyczak E, Wierzbicka A, Jelen HH. Rapid analysis of Baijiu volatile compounds fingerprint for their aroma and regional origin authenticity assessment. Food Chem. 2021;337:128002. https://doi.org/10.1016/j.foodchem.2020.128002.
27. Tian X, Wang J, Ma Z, Li M, Wei Z. Combination of an E-Nose and an E-Tongue for Adulteration Detection of Minced Mutton Mixed with Pork. J Food Quality. 2019;2019:1–10. https://doi.org/10.1155/2019/4342509.
28. Yu S, Huang X, Wang L, Ren Y, Zhang X, Wang Y. Characterization of selected Chinese soybean paste based on flavor profiles using HS-SPME-GC/MS, E-nose and E-tongue combined with chemometrics. Food Chem. 2022;375:131840. https://doi.org/10.1016/j.foodchem.2021.131840.
29. Li X, Yang Y, Zhu Y, Ben A, Qi J. A novel strategy for discriminating different cultivation and screening odor and taste flavor compounds in Xinhui tangerine peel using E-nose, E-tongue, and chemometrics. Food Chem. 2022;384:132519. https://doi.org/10.1016/j.foodchem.2022.132519.
30. Zhang X, Wu H, Yu X, Luo H, Lu Y, Yang H, et al. Determination of Bitterness of Andrographis Herba Based on Electronic Tongue Technology and Discovery of the Key Compounds of Bitter Substances. Molecules. 2018;23(12):3362. https://doi.org/10.3390/molecules23123362.
31. Yang Y, Wei L. Application of E-nose technology combined with artificial neural network to predict total bacterial count in milk. J Dairy Sci. 2021;104(10):10558–65. https://doi.org/10.3168/jds.2020-19987.
32. Ye Z, Liu Y, Li Q. Recent Progress in Smart Electronic Nose Technologies Enabled with Machine Learning Methods. Sensors (Basel). 2021;21(22) https://doi.org/10.3390/s21227620.
33. Fuentes S, Tongson E, Unnithan RR, Gonzalez VC. Early Detection of Aphid Infestation and Insect-Plant Interaction Assessment in Wheat Using a Low-Cost Electronic Nose (E-Nose), Near-Infrared Spectroscopy and Machine Learning Modeling. Sensors (Basel). 2021;21(17) https://doi.org/10.3390/s21175948.
34. Liu H, Li Q, Yan B, Zhang L, Gu Y. Bionic Electronic Nose Based on MOS Sensors Array and Machine Learning Algorithms Used for Wine Properties Detection. Sensors (Basel). 2018;19(1):45. https://doi.org/10.3390/s19010045.
35. Qiu S, Wang J. The prediction of food additives in the fruit juice based on electronic nose with chemometrics. Food Chem. 2017;230:208–14. https://doi.org/10.1016/j.foodchem.2017.03.011.
36. Gong S, Yuan M, Liu Y, Yn Z, Zeng C, Peng C, et al. Application of stable isotopes with machine learning techniques for identifying Aconiti Lateralis Radix Praeparata (Fuzi) geographical origins. Microchem J. 2022;183:108002. https://doi.org/10.1016/j.microc.2022.108002.
37. Zou G, Xiao Y, Wang M, Zhang H. Detection of bitterness and astringency of green tea with different taste by electronic nose and tongue. PLoS One. 2018;13(12):e0206517. https://doi.org/10.1371/journal.pone.0206517.
38. Kobayashi Y, Habara M, Ikezazki H, Chen R, Naito Y, Toko K. Advanced taste sensors based on artificial lipids with global selectivity to basic taste qualities and high correlation to sensory scores.

Sensors (Basel). 2010;10(4):3411–43. https://doi.org/10.3390/s100403411.
39. Chen YP, Cai D, Li W, Blank I, Liu Y. Application of gas chromatography-ion mobility spectrometry (GC-IMS) and ultrafast gas chromatography electronic-nose (uf-GC E-nose) to distinguish four Chinese freshwater fishes at both raw and cooked status. J Food Biochem. 2021:e13840. https://doi.org/10.1111/jfbc.13840.
40. Alpha MOS (n.d.) Heracles Manual. Available online: https://www.alpha-mos.com/smell-analysis-heracles-electronic-nose.
41. Sipos L, Vegh R, Bodor Z, Zaukuu JZ, Hitka G, Bazar G, et al. Classification of Bee Pollen and Prediction of Sensory and Colorimetric Attributes-A Sensometric Fusion Approach by e-Nose, e-Tongue and NIR. Sensors (Basel). 2020;20(23):6768. https://doi.org/10.3390/s20236768.
42. Breiman L, Friedman J, Olshen R, Stone C. Classification and Regression Trees. Wadsworth International Group. Belmont, California1984
43. Breiman L. Random Forests. Machine Learning. 2001;45(1):5–32. https://doi.org/10.1023/A:1010933404324.
44. Rumelhart DE, Hinton GE, Williams RJ. Learning representations by back-propagating errors. Nature. 1986;323(6088):533–6. https://doi.org/10.1038/323533a0.
45. Jiang F, Deng M, Tang J, Fu L, Sun H. Integrating spaceborne LiDAR and Sentinel-2 images to estimate forest aboveground biomass in Northern China. Carbon Balance Manag. 2022;17(1):12. https://doi.org/10.1186/s13021-022-00212-y.
46. Uddin S, Haque I, Lu H, Moni MA, Gide E. Comparative performance analysis of K-nearest neighbour (KNN) algorithm and its different variants for disease prediction. Sci Rep. 2022;12(1):6256. https://doi.org/10.1038/s41598-022-10358-x.
47. Cherif W. Optimization of K-NN algorithm by clustering and reliability coefficients: application to breast-cancer diagnosis. Procedia Computer Science. 2018;127:293–9.
48. Vapnik V, Golowich S, Smola A. Support vector method for function approximation, regression estimation and signal processing. Adv Neural Inform Proc Syst. 1996;9:281–7.
49. Cortes C, Vapnik V. Support-vector networks. Machine Learn. 1995;20(3):273–97. https://doi.org/10.1007/BF00994018.
50. Hossain S, Chow CWK, Hewa GA, Cook D, Harris M. Spectrophotometric Online Detection of Drinking Water Disinfectant: A Machine Learning Approach. Sensors (Basel). 2020;20(22):6671. https://doi.org/10.3390/s20226671.
51. Alpha MOS (n.d.) Heracles Manual. Available online: https://www.alpha-mos.com/smell-analysis-heracles-electronic-nose#arochembase.
52. He C, Wang J, Yin Y, Li Z. Automated classification of coronary plaque calcification in OCT pullbacks with 3D deep neural networks. J Biomed Opt. 2020;25(9):095003. https://doi.org/10.1117/1.Jbo.25.9.095003.
53. Tassone J, Yan P, Simpson M, Mendhe C, Mago V, Choudhury S. Utilizing deep learning and graph mining to identify drug use on Twitter data. BMC Med Inform Decis Mak. 2020;20(Suppl 11):304. https://doi.org/10.1186/s12911-020-01335-3.
54. Mohammadinia A, Saeidian B, Pradhan B, Ghaemi Z. Prediction mapping of human leptospirosis using ANN, GWR, SVM and GLM approaches. BMC Infect Dis. 2019;19(1):971. https://doi.org/10.1186/s12879-019-4580-4.
55. Foroushani AN, Neupane S, De Heredia PP, Pack CC, Sawan M. Spatial resolution of local field potential signals in macaque V4. J Neural Eng. 2020;17(2):026003. https://doi.org/10.1088/1741-2552/ab7321.
56. Li X, Cui L, Tao S, Chen J, Zhang X, Zhang GQ. HyCLASSS: A Hybrid Classifier for Automatic Sleep Stage Scoring. IEEE J Biomed Health Inform. 2018;22(2):375–85. https://doi.org/10.1109/jbhi.2017.2668993.
57. Hall P, Park BU, Samworth RJ. Choice of neighbor order in nearest-neighbor classification. The Annals of Statistics. 2008;36(5):2135–52, 18. https://doi.org/10.1214/07-AOS537.
58. Huang SH, Tung CW. Identification of consensus biomarkers for predicting non-genotoxic hepatocarcinogens. Sci Rep. 2017;7:41176. https://doi.org/10.1038/srep41176.
59. Sung J, Loughin C, Marino D, Leyva F, Dewey C, Umbaugh S, et al. Medical infrared thermal imaging of canine appendicular bone neoplasia. BMC Vet Res. 2019;15(1):430. https://doi.org/10.1186/s12917-019-2180-6.
60. Martini P, Chiogna M, Calura E, Romualdi C. MOSClip: multi-omic and survival pathway analysis for the identification of survival associated gene and modules. Nucleic Acids Res. 2019;47(14):e80. https://doi.org/10.1093/nar/gkz324.
61. Mian QS. Signal-piloted processing and machine learning based efficient power quality disturbances recognition. PLoS One. 2021;16(5):e0252104. https://doi.org/10.1371/journal.pone.0252104.
62. Deng J, Chen W, Wang C, Wang W. Prediction Model for Coal Spontaneous Combustion Based on SA-SVM. ACS Omega. 2021;6(17):11307–18. https://doi.org/10.1021/acsomega.1c00169.
63. Moosavi SM, Chidambaram A, Talirz L, Haranczyk M, Stylianou KC, Smit B. Capturing chemical intuition in synthesis of metal-organic frameworks. Nat Commun. 2019;10(1):539. https://doi.org/10.1038/s41467-019-08483-9.
64. Yus E, Lloréns-Rico V, Martínez S, Gallo C, Eilers H, Blötz C, et al. Determination of the Gene Regulatory Network of a Genome-Reduced Bacterium Highlights Alternative Regulation Independent of Transcription Factors. Cell Syst. 2019;9(2):143–58.e13. https://doi.org/10.1016/j.cels.2019.07.001.
65. Takeda S, Mine Y, Yoshimi Y, Ito S, Tanimoto K, Murayama T. Landmark annotation and mandibular lateral deviation analysis of posteroanterior cephalograms using a convolutional neural network. J Dent Sci. 2021;16(3):957–63. https://doi.org/10.1016/j.jds.2020.10.012.